Spectroscopy and dynamics of excited states in maleimide and N-methyl maleimide: ionic projection and ab initio calculations

ter Steege, D.H.A.; Buma, W.J.

DOI
10.1063/1.1574803

Publication date
2003

Published in
Journal of Chemical Physics

Spectroscopy and dynamics of excited states in maleimide and N-methyl maleimide: Ionic projection and *ab initio* calculations

D. H. A. ter Steege and W. J. Buma[a)]
Faculty of Science, Institute of Molecular Chemistry, University of Amsterdam, Nieuwe Achtergracht 127–129, 1018 WS Amsterdam, The Netherlands

(Received 13 February 2003; accepted 25 March 2003)

The state that is responsible for the strong one-photon absorption around 200 nm in the vapor absorption spectrum of maleimide and N-methyl maleimide has been investigated using excited-state photoelectron spectroscopy in combination with *ab initio* calculations. The projection of the wave function of the excited state on the ionic manifold done in this way reveals multiple, vibrationally resolved, ionization pathways to ground- and excited states of the radical cation, which provide direct evidence for electronic couplings with other, lower-lying states. From a comparison of the experimental intensity distribution over the ionic vibrational states with *ab initio* calculated Franck–Condon factors, we are able to elucidate the role of the various electronically excited states in the ionization process. The experiments also provide the first determination of adiabatic ionization energies in the two molecules. For maleimide values of 10.330 and 10.903 eV are found for D_0 and D_1, respectively; for N-methyl maleimide D_0 is found at 9.897 or, in an alternative interpretation of the spectrum, at 9.676 eV. Calculations and experiment demonstrate that in this molecule the ground ionic state changes its character with respect to maleimide from a lone pair to a π orbital ionization. © *2003 American Institute of Physics.* [DOI: 10.1063/1.1574803]

I. INTRODUCTION

Excited-state photoelectron spectroscopy has in recent years emerged as a powerful means to obtain a detailed characterization of an excited state. Basically, what one does is to project the electronic and vibrational wave function of the excited state onto the rovibronic manifold of the radical cation. Most often this is done employing the ground-state D_0 of the radical cation to provide the basis functions for the projection,[1,2] but other radical cationic states can be used to one's advantage as well (Refs. 3–5, and references therein). Electronic relaxation dynamics is an example of a research area where the projection on one or more electronic ionic states has proven to be particularly rewarding. Time-resolved photoelectron spectroscopy can in these cases provide an excellent view of the internal conversion pathways and the nonadiabatic vibronic couplings that lie at their origin. A recent study of Stolow *et al.* gives in this respect a good overview of what has been done up till now.[5] A useful concept that was introduced in the studies of Stolow *et al.* was that of corresponding[4] and complementary[3] ionization correlations, i.e., the ionization behavior of coupled states that correlate with the same and with different ionic states, respectively.

In most of the time-resolved studies, the *vibrational* resolution in the photoelectron spectrum was of secondary importance; what counted primarily was that one was able to make a distinction between either different ionic states that were accessed in the case of complementary ionization, or differences in the total ionic vibrational content in the case of corresponding ionization. We have demonstrated that the complementary approach of concentrating on the energy resolution in the frequency domain—as opposed to time resolution in the time domain—enables one to disentangle vibronically coupled states as well.[1,2,6] As might be expected, these studies show that the frequency domain approach has its own distinct advantages, in particular for close-lying states that ionize to the same electronic ionic state. Application to complementary ionization channels has, however, not been done so far, but is one of the subjects of interest in the present study on maleimide and N-methyl maleimide.

Photoinduced polymer synthesis is a continuously growing field in which maleimide and its N-substituted derivatives (Fig. 1) have attracted considerable interest. It has been known for quite some time now that N-substituted maleimides easily polymerize by a free-radical polymerization process upon exposure to light.[7] N-substituted maleimides can thus serve as photoinitiators for the free-radical polymerization and copolymerization of a variety of functional species including acrylate, vinyl ether, and styryloxy monomers.[8–17] To give one particular example, in the aerospace industry bismaleimides are widely used because of the advantage they offer density wise, while maintaining mechanical properties that are similar to metal alloys. The first step in initiating the free-radical polymerization reaction with these compounds is excitation of the maleimide chromophore. Intersystem crossing, of which the quantum yield has been shown to be very sensitive to substitution,[18] leads then to population of the lowest excited triplet state. This triplet species reacts with hydrogen atom donors such as alcohols and ethers via direct hydrogen atom abstraction, or with amines and vinyl ethers via an electron-transfer/proton-transfer reaction sequence ini-

a)Author to whom correspondence should be addressed. Electronic mail: wybren@science.uva.nl

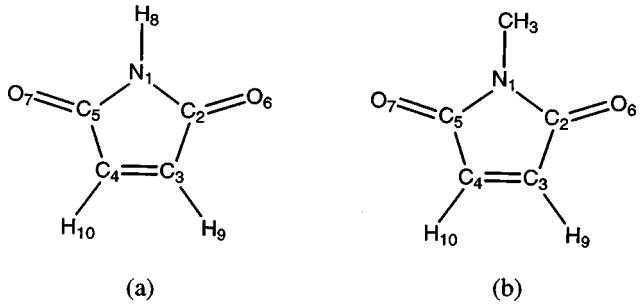

FIG. 1. Molecular structure of (a) maleimide and (b) N-methyl maleimide, as well as employed labeling of atoms.

tiating the free-radical polymerization reaction.[19,20] Maleimide has also been employed in a variety of photochemical applications. One such application is based on the electron accepting properties of maleimide. It has been shown that these properties can form the basis for modulating the fluorescence of compounds in which maleimide is incorporated. This modulation, in turn, can be used to probe polymerization dynamics[21] or as a molecular sensor.[22]

Applications such as the ones mentioned above revolve around the interaction of the molecule with light and involve electronically excited states, and one might therefore assume that the electronic spectroscopy and dynamic properties of the excited states of the molecule and its derivatives would have been studied extensively. The opposite is true. One of the first studies specifically dedicated to the electronic properties of the molecule was done by Matsuo,[23] who claimed that in n-hexane the absorption band of lowest energy was located at about 270 nm, and should be assigned to a $\pi\pi^*$ transition. These results were later revised in a series of studies by Seliskar and McGlynn,[24–26] who found four electronic valence transitions below 6.5 eV. The lowest absorption band of maleimide in apolar solvents was found at 372 nm ($\sim$26 880 cm^{-1}) and assigned as the transition to an $n\pi^*$ state. At higher excitation energies, two more bands were found around 280 and 200 nm that were assigned as $\pi\pi^*$ transitions. Finally, a weak emission starting at 443 nm was found that was attributed to the $T_1 \leftarrow S_0$ transition. From its lifetime, it was concluded that this T_1 state is an $n\pi^*$ state. The N-methyl-substituted compound has also been investigated in these studies. For this molecule two $^1\pi\pi^*$ transitions were reported, the lower-energy one exhibiting a marked redshift ($\sim$3800 cm^{-1}) with respect to its parent compounds, the second one being less sensitive to methyl substitution ($\sim$500 cm^{-1}).

The present study has a twofold aim. On the one hand, we wish to elucidate the spectroscopic properties of the strongest one-photon absorbing state located around 200 nm in maleimide and N-methyl maleimide. To this purpose we have employed $(1+1)$ resonance enhanced multiphoton ionization (REMPI) spectroscopy. Absorption in the 200 nm band populates a higher excited state that is subject to internal conversion processes. The second aim of our studies is to study the underlying vibro–electronic couplings between the various states in the frequency domain by vibrationally resolved excited-state photoelectron spectroscopy. That the maleimide system is particularly adapted for such studies can be anticipated from the results of semiempirical calculations by Seliskar and McGlynn.[26] There it was seen that a limited number of molecular orbitals are important for the description of the lower excited states of the neutral molecule. Preliminary *ab initio* calculations performed by us confirmed this picture: for maleimide of C_{2v} symmetry it was found that the relevant orbitals are the symmetric $n_o^+(a_1)$ and antisymmetric $n_o^-(b_2)$ combinations of the lone pair orbitals on the oxygen atoms, a C=C bonding π orbital (b_1) that we will label as $\pi_{C=C}$, a π orbital (b_1) that has a dominant contribution from the nitrogen atom and is labeled as π_N, and an antibonding π^* orbital (a_2). The lower excited singlet states are then in first approximation described by the $(\pi^* \leftarrow n_o^-)$ excitation (S_1), the $(\pi^* \leftarrow n_o^+)$ excitation (S_2), while the $\pi\pi^*$ states S_3 and S_4 are described by combinations of the $(\pi^* \leftarrow \pi_{C=C})$ and $(\pi^* \leftarrow \pi_N)$ excitations. Although we do not yet know anything on the ordering and composition of the electronic states of the radical cation, it is reasonable to expect that when these configurations are ionized, each of them is associated with a unique ionic state: S_1 correlates with the $(n_o^-)^{-1}$ state, S_2 with the $(n_o^+)^{-1}$ state, while S_3 and S_4 correlate with states based upon the $(\pi_N)^{-1}$ and $(\pi_{C=C})^{-1}$ configurations.

The state associated with the strong 200 nm absorption is the $S_4(\pi\pi^*)$ state. The above considerations lead to the conclusion that, if this state is coupled to any of the lower-lying states, one might distinguish the contributions to the (coupled) wave function by selection of the appropriate ionization channel. Coupling to S_1—or, in the time domain, internal conversion to this state—for example, should become visible by population of the $(n_o^-)^{-1}$ ionic state, which is not accessible from S_4. On the basis of their electronic description, we can anticipate that the equilibrium geometry and force fields of the states of interest (S_1 to S_4) are different. This implies that if ionization of the contributing states in the coupled wave function would take place to the same ionic state, one might still distinguish the various contributions by their gross vibrational content, but in particular by the Franck–Condon pattern in a vibrationally resolved photoelectron spectrum. The experimental results that are obtained by excited-state photoelectron spectroscopy will therefore be combined with extensive *ab initio* calculations. It will be shown that we can characterize in this way in quite some detail the spectroscopic and dynamic properties of the strongly absorbing $\pi\pi^*$ state of maleimide and N-methyl maleimide. Apart from elucidating the electronic structure of the neutral molecules, the present study provides us with an comprehensive view on the electronic structure of the radical cation of the two species.

II. EXPERIMENTAL AND THEORETICAL DETAILS

The experiments reported in this study have been performed using a setup that has been described in detail before.[27,28] Here, we will therefore only summarize some of the aspects that are relevant for the present experiments. The laser setup consists of a pulsed dye laser (Lumonics Hyperdye-300) running on Coumarine 440, which is pumped

by a XeCl excimer laser (Lambda Physik EMG103-MSC). The excimer laser gives 10 ns pulses with a maximum pulse energy of 200 mJ and is predominantly used at a repetition rate of 30 Hz. The dye laser output with a spectral bandwidth of about 0.07 cm^{-1} was frequency doubled using an angle-tuned BBO crystal in an INRAD Autotracker II unit, and focused into the ionization region of the magnetic bottle spectrometer[29] that is interfaced with a molecular beam expansion.[27] So far, we have employed this spectrometer in experiments in which an excited state is predominantly populated by absorption of more than one photon, and therefore used a lens with a focal length of 25 mm. In the present experiments one-photon excitation is used, for which a 25 mm lens gave rise too easily to saturation effects. The 25 mm lens was therefore replaced by a 225 mm lens. Theoretically, this might give rise to a worse resolution in the photoelectron spectra (*vide infra*)[29] because of the large focal volume, but in practice we could still obtain the same—or slightly worse—resolution as became clear from calibration experiments on xenon.

In order to have enough vapor pressure of the compound under investigation, the sample is put into a sample container that can be heated. When the sample needs to heated, the temperature of the 0.5 mm nozzle (General Valve Iota One System) is normally kept 10 °C higher than the sample container in order to avoid condensation in the injector. N-methyl maleimide has a vapor pressure at room temperature of >200 mTorr, and, when heated up to 90 °C, was not difficult to study under supersonic beam conditions. Maleimide, on the other hand, has a negligible vapor pressure at room temperature. Upon heating we could observe some signal under supersonic beam conditions, but not enough to record excited-state photoelectron spectra of good enough quality. We have therefore also performed experiments on effusively introduced samples. In those experiments the sample did not need to be heated, because enough vapor pressure was generated by simply pumping on the sample. Maleimide and N-methyl maleimide were obtained from Aldrich and employed as supplied.

Excitation spectra have been constructed by integration of (part of) the photoelectrons over the scanned wavelength region. Photoelectron spectra have been recorded by increasing in steps the retarding voltage on a grid surrounding the flight tube, and transforming each time only the high-resolution part of the time-of-flight spectrum. For wavelengths above ~240 nm the photoelectron peaks have widths of about 10 meV at all kinetic energies. For shorter wavelengths, the resolution becomes progressively worse to such an extent that near 225 nm—the wavelength region employed in the present experiments—the width of the photoelectron peaks increases to about 25 meV. The energy scale of the photoelectrons as well as the laser wavelengths were calibrated using multiphoton resonances of krypton or xenon.[30]

Density functional theory (DFT) and time-dependent DFT (TD–DFT) calculations on the ground-and excited states of maleimide and N-methyl maleimide in its neutral and radical cationic form have been performed employing the GAUSSIAN 98 suite of programs.[31] For the complete active space self-consistent-field (CASSCF) calculations on the excited states of maleimide, the GAMESS-DAKOTA package has been used.[32] Franck–Condon factors have been evaluated with an in-house-written program[33] that is based upon the methods developed by Doktorov *et al.*[34]

TABLE I. Geometrical parameters (Å and degrees) of maleimide in its neutral and ionic ground state.

	S_0 Experiment[a]	S_0 B3LYP/6-311+G*	D_0 UB3LYP/6-311+G*
H–C	1.096[b]	1.081	1.082
H–N	1.025[b]	1.009	1.017
C═C	1.344	1.334	1.323
C–C	1.508	1.503	1.517
C–N	1.409	1.396	1.394
C═O	1.206	1.206	1.199
C–N–C	112.0	111.8	109.4
N–C–C	106.8	105.1	107.0
N–C═O	123.9	126.4	123.1
$C_5-C_4-H_{10}$[c]		121.7	120.8

[a]From Ref. 39.
[b]Assumed parameters in Ref. 39.
[c]Reference 39 reports a C–C–H angle of 114.7°, but it is not clear from the paper which angle is reported. Reference 48 reports an electron diffraction study in which an average value of 125.5° is obtained for the $C_9-C_{10}-H_8$ angle, but in the crystal the geometry of the molecule is affected by intermolecular hydrogen bonds and dimeric interactions.

III. RESULTS AND DISCUSSION

In the following we will present and discuss the excitation and photoelectron spectra that have been obtained for maleimide and N-methyl maleimide in the energy region where the strong aborption to the $2\,^1B_1$ ($\pi\pi^*$) state is located. As we have demonstrated amply before,[1,2,6,35] an optimal analysis of photoelectron spectra requires knowledge of the vibrational frequencies in the ionic state to which ionization occurs. As yet, however, virtually nothing is known about these frequencies, but our experience is that—at least for the ground state of the radical cation—an accurate enough prediction can be obtained from density functional theory calculations. During the analysis of our results, it also became clear that not only an accurate description of the ground electronic state of the radical cation was needed, but of the excited states of the neutral molecule and of the radical cation as well. Prior to discussing the experimental results, we will therefore in the next sections present the results of our *ab initio* calculations, and subsequently use them to guide the interpretation of our experimental results.

A. Maleimide

1. Ab initio calculations

Optimization of the molecular geometry of maleimide in its electronic ground state S_0 at the B3LYP/6-311+G*[36–38] level leads to a C_{2v} structure with structural parameters reported in Table I. Good agreement is observed with parameters as determined in an electron diffraction study of maleimide in the gas phase.[39] The electronic configuration at this geometry is given by $\cdots(2b_1)^2\ (12a_1)^2(3b_1)^2\ (9b_2)^2$. From the orbital contour plots shown in Fig. 2, it is seen that the relevant π orbitals of b_1 symmetry can roughly be char-

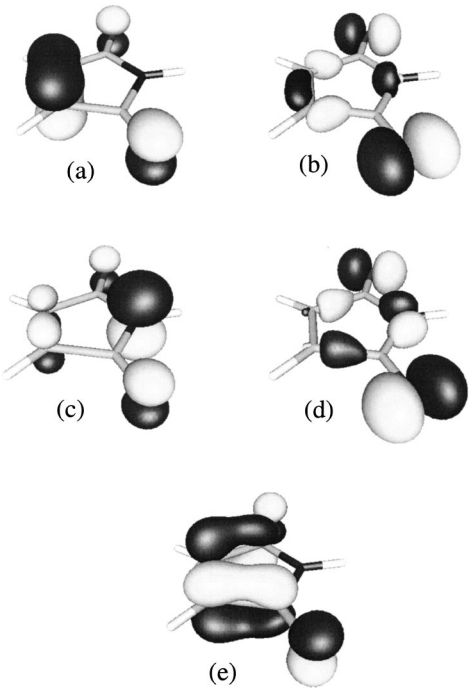

FIG. 2. Contour plots of the (a) $2b_1$ ($\pi_{C=C}$), (b) $12a_1$ (n_o^+), (c) $3b_1$ (π_N), (d) $9b_2$ (n_o^-), and (e) $2a_2$ (π^*_{C-C}) molecular orbitals of maleimide.

acterized as being localized on the nitrogen atom ($2b_1 = \pi_{C=C}$) and the C=C bond ($3b_1 = \pi_N$). The in-plane $12a_1$ and $9b_2$ orbitals consist of the symmetric and antisymmetric combination of the oxygen lone pair orbitals, respectively, and will be designated as n_o^+ and n_o^-. In the following, we will see that the lower-lying excited states of interest in the present studies are in first approximation described as excitations of electrons from these π- and n orbitals to the $2a_2(\pi^*)$ orbital. The contours of this virtual orbital, which will be designated as π^*_{C-C}, are depicted in Fig. 2, and show that it is characterized by bonding C–C and antibonding C=C character.

The ground state D_0 of the radical cation derives in our calculations from the removal of an electron from the $9b_2(n_o^-)$ orbital, resulting in a state of $^2B_2$ symmetry. Optimization of the geometry of the molecule in this state results in a structure with C_{2v} symmetry and structural parameters that are given in Table I. In line with the nonbonding character of the n_o^- orbital, the geometry of the molecule is hardly affected by the removal of an electron from this orbital.

The vibrational frequencies obtained from the calculation of the harmonic force field for both states are listed in Table II. For the ground state of the neutral molecule excellent agreement is found between (scaled) calculated values and experimental frequencies determined by infrared and Raman spectroscopy.[40–42] For the ground state of the radical cation, vibrational frequencies have not yet been determined experimentally.

To investigate the excited-state manifold of the neutral and radical cation, we have used time-dependent density functional theory calculations at their (U)B3LYP/6-311 +G* optimized geometries, once again with the B3LYP

TABLE II. Experimental and *ab initio* vibrational frequencies (cm^{-1}) of ground and ionic states of maleimide.

Symmetry	Mode	S_0[a] B3LYP	S_0[b] Experiment	D_0[a] UB3LYP	Description[c]
a_1	ν_1	3536	3482	3447	νN–H
	ν_2	3145	3090	3147	νC–H
	ν_3	1793	1775	1719	νC=O
	ν_4	1592	1580	1584	νC=C
	ν_5	1295	1335	1173	νC–N–C
	ν_6	1045	1067[d]	1044	δC–H
	ν_7	874	897	822	νC–C
	ν_8	621	637	609	Ring deformation
	ν_9	380	415[d]	360	δC=O
a_2	ν_{10}	940	972[d]	851	γC–H
	ν_{11}	758	776[d]	581	Ring deformation
	ν_{12}	287	301[d]	276	γC=O
b_1	ν_{13}	821	831	792	γC–H
	ν_{14}	616	721[d]	596	νN–H
	ν_{15}	522	635[d]	517	Ring deformation
	ν_{16}	135	175[d]	149	γC=O
b_2	ν_{17}	3124	3108[d]	3129	νC–H
	ν_{18}	1758	1756	1508	νC=O
	ν_{19}	1318	1322	1313	δN–H
	ν_{20}	1277	1285	1220	δC–H
	ν_{21}	1092	1130	907	νC–N–C
	ν_{22}	888	906	649	Ring deformation
	ν_{23}	651	668	611	Ring deformation
	ν_{24}	520	504	475	δC=O

[a]After scaling with factor 0.9676 (Ref. 49).
[b]Vapor phase values taken from Ref. 40, except those labeled d.
[c]Description appropriate for S_0; ν=stretch; δ=in-plane bend; γ=out-of-plane bend.
[d]Raman values taken from Ref. 40.

TABLE III. Description of the ground- and lower-lying electronic excited states of neutral maleimide and of the ground and first excited states of its radical cation. For the singlet states of the neutral molecule, vertical excitation energies and oscillator strengths have been calculated by TD–DFT at the B3LYP/6-311+G* optimized S_0 ($1\,^1A_1$) geometry; for the radical cation excitation energies have been calculated by TD–DFT at the UB3LYP/6-311+G* optimized geometry of the D_0 ($X\,^2B_2$) state of the radical cation. The adiabatic excitation energy of the T_1 ($1\,^3B_1$) state was calculated at the UB3LYP/6-311+G* level.

State	Description	Energy (eV)	Oscillator strength
S_0 ($1\,^1A_1$)	$(\pi_{C=C})^2(n_o^+)^2(\pi_N)^2(n_o^-)^2$	0	
S_1 ($1\,^1B_1$)	$(\pi_{C=C})^2(n_o^+)^2(\pi_N)^2(n_o^-)^1(\pi^*_{C-C})^1$	3.46	0.0000
S_2 ($1\,^1A_2$)	$(\pi_{C=C})^2(n_o^+)^1(\pi_N)^2(n_o^-)^2(\pi^*_{C-C})^1$	4.23	0.0000
S_3 ($1\,^1B_2$)	$(\pi_{C=C})^2(n_o^+)^2(\pi_N)^1(n_o^-)^2(\pi^*_{C-C})^1$	4.51	0.0046
S_4 ($2\,^1B_2$)	$(\pi_{C=C})^1(n_o^+)^2(\pi_N)^2(n_o^-)^2(\pi^*_{C-C})^1$	5.77	0.3222
T_1 ($1\,^3B_1$)	$(\pi_{C=C})^2(n_o^+)^2(\pi_N)^2(n_o^-)^1(\pi^*_{C-C})^1$	2.84	
D_0 ($X\,^2B_2$)	$(\pi_{C=C})^2(n_o^+)^2(\pi_N)^2(n_o^-)^1$	0	
D_1 ($A\,^2B_1$)	$-0.69\,(\pi_{C=O})^2(\pi_{C=C})^1(n_o^+)^2(\pi_N)^2(n_o^-)^2$ $+0.82\,(\pi_{C=O})^2(\pi_{C=C})^2(n_o^+)^2(\pi_N)^1(n_o^-)^2$	0.63	
D_2 ($B\,^2B_1$)	$0.85\,(\pi_{C=O})^2(\pi_{C=C})^1(n_o^+)^2(\pi_N)^2(n_o^-)^2$ $+0.62\,(\pi_{C=O})^2(\pi_{C=C})^2(n_o^+)^2(\pi_N)^1(n_o^-)^2$	0.93	

functional. For the four lower excited states of the neutral molecule electron configurations, excitation energies and oscillator strengths are reported in Table III. We find that the first excited singlet state ($1\,^1B_1$) is an $n\pi^*$ state obtained by excitation of an electron from the n_o^- to the π^*_{C-C} orbital. The essentially forbidden $1\,^1B_1 \leftarrow 1\,^1A_1$ transition has a calculated transition energy of 3.46 eV (27 900 cm^{-1}), which agrees very well with the study of Seliskar and McGlynn, in which a very weak $n\pi^*$ transition at ~360 nm (3.3 eV) was reported.[24] The second excited singlet state, $1\,^1A_2$, is a one-photon symmetry-forbidden $n\pi^*$ transition described by excitation of an electron from the n_o^+ orbital to the π^*_{C-C} orbital. The third and fourth excited singlet states are of $\pi\pi^*$ character, with S_3 ($1\,^1B_2$) being dominated by the $\pi_N \rightarrow \pi^*_{C-C}$ configuration and S_4 ($2\,^1B_2$) by the $\pi_{C=C} \rightarrow \pi^*_{C-C}$ configuration. Experimentally, two $\pi\pi^*$ transitions have been observed with vertical excitation energies of 4.4 and 5.9 eV, respectively. These excitation energies compare well with the values of 4.51 and 5.77 eV obtained in our calculations. For the $S_4 \leftarrow S_0$ transition, experimental and predicted values of the oscillator strength are in excellent agreement (0.31 vs 0.32). The calculations predict a small oscillator strength for the transition to S_3, while experimentally a value of 0.24 was reported. This latter value seems rather high considering that molar extinction coefficients of 750 and 10 000 $M^{-1}\,cm^{-1}$ were found for the S_3 and S_4 transitions, respectively. The reason for the discrepancy between the experimental and calculated values of the oscillator strength of the transition to S_3 is not clear, but for the present discussion not directly important. One other state of interest to the present study that has been investigated in the past is the lowest excited triplet state T_1. TD–DFT as well as UB3LYP calculations find this state to be the $1\,^3B_1$ ($n_o^+\pi^*_{C-C}$) state with an adiabatic excitation energy of 2.84 eV (~23 000 cm^{-1}), which is in excellent agreement with the experimentally observed value.

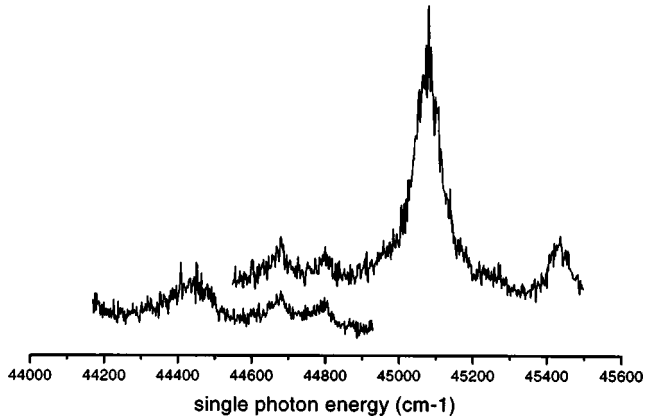

FIG. 3. (1+1) REMPI excitation spectrum of effusively introduced maleimide. The spectrum consists of two scans that have been displayed vertically for reasons of clarity.

For the radical cation we are in the present study mainly interested in the ground-and first excited state. The ground state D_0 ($X\,^2B_2$) is described by removal of an electron from the n_o^- orbital. Our calculations predict, for the vertical and adiabatic ionization energies to D_0, values of 10.286 and 10.219 eV, respectively. The relatively small difference of 67 meV is in agreement with our conclusion above on the (nonbonding) character of the n_o^- orbital. Experimental values for the ionization energy of maleimide have thus far not been reported, but the calculated value is not in disagreement with the value of 9.991 eV that has been reported for the vertical ionization energy of N-methylmaleimide[43] (see also below, however). The first excited state in the ionic manifold is the $A\,^2B_1$ state, predicted to lie 0.63 eV above the $X\,^2B_2$ state. This state is largely about an 1:1 mixture of configurations with a hole in the $\pi_{C=C}$ or in the π_N orbital. Its counterpart is the second excited $B\,^2B_1$ state, which is located 0.93 eV above the ionic ground state.

2. Multiphoton ionization and excited-state photoelectron spectroscopy

A (1+1) REMPI excitation spectrum of maleimide, introduced effusively in the spectrometer, was recorded in the 44 000–45 500 cm^{-1} spectral region, and is shown in Fig. 3. On the basis of previous absorption measurements and our *ab initio* calculations, we expect to see here the transition to the $2\,^1B_2(\pi\pi^*)$ state, and consequently assign the resonance at 45 070 cm^{-1} as the vibrationless transition to this state. Compared with the same transition in N-methyl maleimide[43] (see also Sec. III B 2), this implies a blueshift of 480 cm^{-1}, which is what may be expected for the effect of methylation. Apart from the origin transition, four more transitions are observed. The bands observed at 635 and 395 cm^{-1} to the red of the 0_0^0 transition are readily assigned to the 8_1^0 and 9_1^0 hot band transitions on the basis of the frequencies reported in Table I. The same table shows that the band shifted by 280 cm^{-1} to the red cannot be assigned to an a_1 vibration. Although this frequency is similar to that of ν_{12} in the ground state, it is hard to imagine that it would be the 12_1^0 hot band, because that would imply loss of symmetry in the excited state, and lead us to expect that the 12_0^1 transition

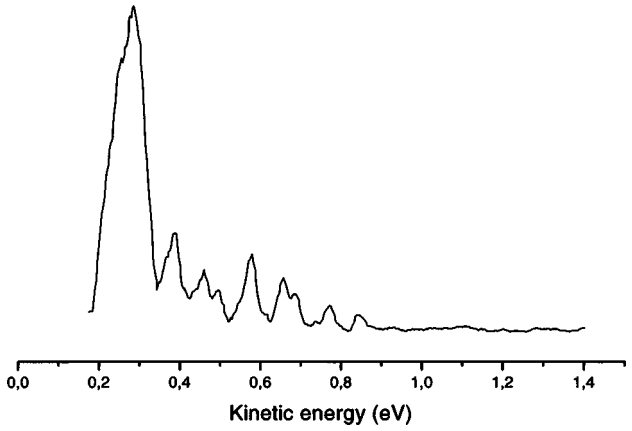

FIG. 4. Excited-state photoelectron spectrum of the vibrationless S_4 excited state of maleimide excited at 45 070 cm^{-1}.

TABLE IV. Assignments of peaks observed in excited-state photoelectron spectrum displayed in Fig. 4 that was obtained at the 0–0 transition to S_4 (45 075 cm^{-1}).

Electron kinetic energy (eV)	Ion internal energy (cm^{-1})	Assignment
0.846	0	$0''-0^+$ (D_0)
0.772	597	8^1
0.739	863	7^1
0.688	1274	8^2 (or 5^1)
0.656	1532	4^1 (or 8^17^1)
0.618	1839	8^3 (or 3^1 or 5^18^1)
0.575	2186	4^18^1
0.493	2847	4^18^2
0.458	3129	4^2
0.382	3742	4^28^1
0.273	0	$0''-0$ (D_1)

would also be observable. It is more probable that this band is associated with a $(\nu_i)_1^1$ transition, implying that one of the modes undergoes a rather dramatic frequency decrease upon excitation, but which mode cannot be determined. The resonance at 45 435 cm^{-1} is assigned as the 9_0^1 transition. The observed frequency decrease in the excited state is in line with an increased antibonding character of the C═O bond upon excitation (see Fig. 2).

The photoelectron spectrum recorded at the 0–0 transition to the S_4 state is depicted in Fig. 4. Before assigning the various peaks in this spectrum, it is instructive to think of what we may expect to see on the basis of the electronic composition of the excited state. Our *ab initio* calculations have shown that the dominant configuration in the wave function of S_4 is the $\pi_{C=C}\rightarrow\pi^*_{C-C}$ configuration. From these calculations we have also seen that D_0 is described as the $(n_o^-)^{-1}$ state. Within this simple one-configuration picture, ionization of S_4 to D_0 is thus in first approximation forbidden. Ionization to the D_1 and D_2, states, which in the same picture are described by a combination of the $(\pi_N)^{-1}$ and $(\pi_{C=C})^{-1}$ configurations, is on the other hand, fully allowed. The *ab initio* calculations therefore predict that the dominant ionization pathways of S_4 are to D_1 and D_2, and not to D_0.

The peak with the highest photoelectron energy in Fig. 4 is found at 0.846 eV. Normally, one would assume that this peak is the $0''-0_0^+$ peak, i.e., that it derives from an ionization process that starts in the vibrationless ground state and ends up in the vibrationless D_0 ionic state, but the discussion above indicates that in the present case such an assignment is not that straightforward. Nevertheless, the value of 0.846 eV leads to an ionization energy of 10.330 eV, which agrees very well with the *ab initio* predicted adiabatic value for D_0 (10.22 eV), and we therefore assign this peak as the $0''-0_0^+$ band. The strongest peak in the spectrum occurs at a photoelectron energy of 0.273 eV. Its width, which is significantly larger than the experimental resolution, indicates that it consists of various unresolved transitions. If this peak were to be associated with ionization to D_0, it would mean that ions are formed with an internal energy of 0.573 eV, and, considering its intensity relative to the $0''-0_0^+$ band, one would have to conclude that the molecule is subject to very large geometry changes upon ionization. An alternative explanation is suggested by the previous discussion on the ionization pathways of S_4, namely, that this peak derives from ionization to D_1. Our calculations predict the $0''-0_1^+$ peak to appear with 0.63 eV less energy than the $0''-0_0^+$ peak. The position and intensity of the 0.573 eV peak are therefore in good agreement with its assignment as the $0''-0_1^+$ transition, and allow us to conclude that the adiabatic ionization energy to D_1 is 10.903 eV. From a configurational point of view, ionization to D_2 is also allowed. This pathway is not observed in the photoelectron spectrum, which is in line with the calculations that predict this state to be 0.3 eV higher in energy than D_1, and thus energetically not accessible in the present one-color experiments.

The spectrum displays a significant amount of other activity. Assuming that the molecule retains C_{2v} symmetry upon excitation, and that the ionization step can be described within the Born–Oppenheimer approximation, these bands should be associated with ionization to totally symmetric vibrational levels in the ion. As Table IV shows, we find indeed that it is not difficult to assign the spectrum in terms of ionization to vibrational levels of D_0 that involve predominantly the ring deformation mode ν_8^+ and the C═C stretching vibration ν_4^+. At the same time, it should be remarked that the resolution in the spectrum does not rule out other assignments as indicated as well for some of the entries in the same table. A possible explanation for the D_0 activity is direct two-photon ionization of the ground state. This can be excluded experimentally by observing that the D_0 ionization pathway is only present when resonance occurs with S_4. Theoretically, it is seen that the calculated Franck–Condon factors (*vide infra*) for the $D_0+e^-\leftarrow S_0$ transition, which are given in Table V, are at odds with the observed intensity distribution in the photoelectron spectrum.

In the simple model discussed above, ionization of S_4 to $D_0$is forbidden. Nevertheless, we have now concluded that the photoelectron spectrum gives evidence for a nonnegligible role of ionization to D_0. A number of explanations come to mind. The first is that the model is too simple and that $D_0\leftarrow S_4$ ionization is allowed in higher order. In that case, the vibrational intensity distribution in the photoelec-

TABLE V. Franck–Condon factors between the vibrationless level of various electronic states of maleimide and fundamental levels of totally symmetric vibrations in the ground ionic state D_0. The equilibrium geometry and harmonic force field of S_0 and D_0 have been obtained at the (U)B3LYP/6-311+G* level, while for S_1, S_2, S_3, S_4, T_1, and T_4 the CAS calculations described in the text have been employed.

Vibration	Frequency (cm^{-1})[a]	$D_0 \leftarrow S_0$[b]	$D_0 \leftarrow S_1$[b]	$D_0 \leftarrow S_2$[b]	$D_0 \leftarrow S_3$[b]	$D_0 \leftarrow S_4$[b]	$D_0 \leftarrow T_1$[b]	$D_0 \leftarrow T_4$[b]
ν_9^+	360	40.0	6.1	7.1	2.0	0.5	4.7	13.5
ν_8^+	609	35.3	29.6	55.0	359.4	71.0	26.9	51.0
ν_7^+	822	8.6	146.1	153.3	143.7	129.6	138.4	144.3
ν_6^+	1044	1.5	4.4	10.8	23.6	19.5	3.3	9.3
ν_5^+	1173	2.7	25.4	19.8	317.9	8.4	21.3	14.6
ν_4^+	1584	2.8	117.0	192.4	22.6	154.5	95.2	167.5
ν_3^+	1719	0.0	75.3	148.2	39.7	32.5	62.8	130.6
ν_2^+	3147	0.0	2.5	2.6	3.8	3.3	2.3	2.4
ν_1^+	3447	0.2	2.6	2.8	1.4	2.0	2.6	2.8

[a]After scaling with factor 0.9676 (Ref. 49).

[b]Intensity of transition from 0^0 level in excited state to $\nu_i^+(a_1)=1$ level in ionic state. Intensity is given with respect to intensity of $0^{0+} \leftarrow 0^{0\prime}$ transition, which has been taken as 100.0.

tron spectrum should be proportional to the Franck–Condon factors between the vibrationless level of S_4 and ionic vibrational levels, assuming of course that the $D_0+e^- \leftarrow S_4$ electronic transition moment is more or less independent of the vibrational coordinates. To investigate this hypothesis, we have determined the C_{2v} equilibrium geometry of the molecule in S_4 at the CASSCF/6-311G* level. The active space in these calculations consisted of the already-mentioned n_o^+, n_o^-, π_N, $\pi_{C=C}$, and π^*_{C-C} orbitals, augmented with the $1b_1$ and $1a_2$ π-, and the $4b_1$ and $3a_2$ π^*-orbitals. Franck–Condon factors were then calculated from the displacement parameters with respect to the UB3LYP/6-311+G* equilibrium geometry of the D_0 state. We notice that in this approximation of the Franck–Condon factors, normal-mode rotations upon ionization are not taken into account. However, our goal at this point is to obtain qualitative agreement between experiment and theory, and because Franck–Condon factors are primarily determined by geometry changes, inclusion of normal-mode rotations is not expected to lead to major changes in the results.

The results of these calculations are shown in Table V, where the intensities for transitions from the 0^0 level in S_4 to fundamental vibrational levels of a_1 modes in D_0 are given. They show that for ionization of S_4 to D_0 dominant activity is expected in the ν_8^+ (ring deformation), ν_7^+ (C–C stretch), and ν_4^+ (C=C stretch) modes. This agrees with the experiment insofar as ν_8^+ and ν_4^+ are concerned, but the large difference between predicted and experimental activity of ν_7^+ is distressing. Moreover, we notice that the intensity distribution in the photoelectron spectrum in Fig. 4—if attributed to ionization of a single vibrationless excited state level—can only be understood if the excited- and ionic state have very different equilibrium geometries. This is not supported by the calculated Franck–Condon factors.

The conclusion that the observed D_0 activity cannot be reconciled with a mere ionization of the vibrationless level of S_4 means that the D_0 activity must at least in part also be associated with the ionization of another state. This implies that the ''bright'' S_4 state, responsible for the intensity in the absorption step, is coupled to ''dark'' levels of another state, which give rise to D_0 activity upon ionization. At this point it is not clear to which lower-lying electronic state(s) coupling occurs, but what is interesting is that vibrational resolution is still maintained in the ionization step to D_0 despite the large energy gaps with the other states (see Table III). Because of these large energy gaps, one expects to deal with nonradiative processes in the statistical limit which populate many vibrational levels, and in general lead to broad and unresolved peaks (see, for example, Refs. 44 and 45). Here we see, however, photoelectron peaks with instrument-limited widths.

The first excited singlet state S_1 is a possible candidate for the state that is coupled to S_4. This state is attractive for two reasons. First, S_1 is in first approximation described by the $\pi^*_{C-C} \leftarrow n_o^-$ excitation and consequently has D_0 $((n_o^-)^{-1})$ as its associated ionizing state. Second, the S_1 state has more than 2.5 eV of vibrational energy at the 0–0 transition energy to S_4, and the state density—and thus possibilities to couple the two states—is huge. One problem in checking this hypothesis is that we do not know which vibrational levels of S_1 are coupled to the 0^0 level of S_4. Even so, it is reasonable to expect that the active vibrations in the photoelectron spectra of these levels are those that are associated with the differences in the equilibrium geometries of the S_1 and D_0 states. A measure for their activities is given by the $I[(\nu_i^+)_0^1]/I[0_0^0]$ ratios, which have been calculated in the same way and at the same level as described above for S_4. The results given in Table V show that for S_1 an ionization behavior is expected that is qualitatively similar to that of S_4. A mere ionization of high-lying vibronically coupled levels of S_1 is thus also concluded to be an unlikely explanation for the observed D_0 ionization pathway.

Although the first-order description of both states seems to exclude direct ionization to D_0, we have also considered the scenario that vibronic coupling occurs with high-lying vibrational levels of S_2 or S_3. Optimization of the C_{2v} geometry of the molecule in these two states, and the subsequent Franck–Condon calculation leads to $I[(\nu_i^+)_0^1]/I[0_0^0]$ intensities that are given in Table V. Apart from an enhanced ν_3^+ activity, the ionization of S_2 gives rise to qualitatively the

same Franck–Condon distribution—and thus objections—that was found for S_4 and S_1, i.e., strong activity of ν_7^+ and ν_4^+, and a smaller activity of ν_8^+. Importantly, Table V reveals that ionization of S_3 is associated with a fundamentally different Franck–Condon behavior. Here, a large activity of ν_8^+ and a smaller activity of ν_7^+ is predicted, but now the activity of ν_4^+ has disappeared and has been replaced by an activity of ν_5^+ that is as large as that of ν_8^+.

For maleimide it has been shown that the triplet quantum yield is close to unity.[18] Intersystem crossing might thus populate highly excited levels of a lower-lying triplet state, which are subsequently ionized into the D_0 ionization continua. For experiments on a nanosecond time scale such behavior has, for example, been observed after excitation of the lowest excited singlet state of pyrazine.[46] The state that is excited in the present experiments is a $\pi\pi^*$ state for which spin–orbit coupling with the lower-lying $T_1(1\,^3B_1)$ and $T_4(1\,^3A_2)$ $n\pi^*$ states is dominant. *A priori* one does, however, not expect that the ionization of these two states leads to Franck–Condon patterns that are much different from the ionization of their singlet counterparts, an expectation that is confirmed by and large by the calculated Franck–Condon factors in Table V. Also, ionization of triplet states is therefore not able to account for the observed intensity distribution in the photoelectron spectrum.

We thus have to conclude that the D_0 activity can only be interpreted consistently if ionization occurs from more than one electronically excited state, or, in other words, from a mixed state that contains the character of various excited states. We do not claim that our calculations and experiments enable us to make a clear distinction between the contributions of the S_1, S_2, S_4, T_1, and T_4 states; they all give rise to a dominant activity of ν_7^+ and ν_4^+ with relatively slight variations in intensities. The latter activity is confirmed by the experiment, and leads us to conclude that one or more of these states is involved in the ionization pathway to D_0. However, at the same time our experiments show unambiguously a major activity of ν_8^+ and a minor activity of ν_7^+, a pattern that can only be explained if ionization of S_3 levels is taken into account. This conclusion implies (i) that more than one state is ionized; and (ii) that ionization of S_3 should be considered beyond a simple one-configuration picture, a conclusion that also needs to be drawn in order to account for the ionization of contributing levels of S_4, S_2, and T_4.

B. N-methyl maleimide

1. Ab initio calculations

Calculations on N-methyl maleimide have been performed under the restriction of C_s symmetry with the mirror plane perpendicular to the ring. Optimization of the molecular geometry in C_s symmetry at the B3LYP/6-311+G* level leads to a ground-state structure of the neutral molecule with structural parameters reported in Table VI, while the vibrational frequencies obtained from the harmonic force field at this geometry are given in Table VII. This table shows that the restriction of C_s symmetry leads to one imaginary frequency. Since it is associated with the rotation of the methyl group, it is not of direct importance for our discussion on the electronic properties of excited and ionic states, and we will therefore just accept it as it is.

TABLE VI. Geometrical parameters (Å and degrees) of N-methyl maleimide in its neutral and ionic ground state.

	S_0 B3LYP/6-311+G*	D_0 UB3LYP/6-311+G*
H–C	1.081	1.083
N–CH_3	1.453	1.417
C═C	1.333	1.349
C–C	1.503	1.479
C–N	1.397	1.481
C═O	1.208	1.187
C–N–CH_3	124.7	125.4
C–N–C	110.5	109.2
N–C–C	106.0	104.3
N–C═O	125.9	122.3
C_5–C_4–H_{10}[a]	121.8	121.4

[a]Same angle as employed in maleimide.

Inspection of the contour plots of the relevant orbitals (not shown) reveals that the methyl substitution on the nitrogen atom hardly influences the electron distribution in the $\pi_{C=C}$, n_o^+, n_o^-, and π^*_{C-C} orbitals. The π_N orbital, on the other hand, obtains a significant (antibonding) density in the π orbital of the carbon atom of the methyl group. Concurrently, the calculations predict that the ground state of the radical cation is no longer associated with the $(n_o^-)^{-1}$ configuration, but becomes the $X\,^2A'$ state, described in first approximation by the removal of an electron from the π_N orbital. The UB3LYP/6-311+G* optimized geometry of the molecule in this $X\,^2A'$ state is reported in Table VI, the vibrational frequencies deriving from the harmonic force field calculation in Table VII. Since ionization to D_0 now occurs from an orbital that has distinct bonding and antibonding characteristics—as opposed to maleimide, where an essentially nonbonding electron was removed—it is seen from Table VI that the geometry changes considerably upon ionization. In agreement with the antibonding density between the nitrogen atom and the methyl group in the ground state, this bond becomes shorter upon ionization. What is also important to notice is the large change in the C–N bond length, which can be interpreted as giving evidence for a large contribution of the Zwitter-ionic resonance structure in the ground state of the neutral molecule.

The results of TD–DFT calculations on the ground- and excited states of the neutral molecule are reported in Table VIII. In agreement with our qualitative conclusion that it was only the π_N orbital that was dominantly affected by the N-methyl substitution, we observe that the ordering and character of most of the lower-lying excited states remains the same, and that only minor changes on the order of 0.1 eV occur in the vertical excitation energy. This is not true for the $(\pi_N \rightarrow \pi^*_{C-C})$ state, which is redshifted by more than 0.5 eV with respect to maleimide and now becomes S_2 instead of S_3. The calculated excitation energies and oscillator strengths are in good agreement with what has been observed previously in absorption spectroscopy on N-methyl maleimide in the gas phase.[24] That study reported two absorption

TABLE VII. Experimental and *ab initio* vibrational frequencies (cm^{-1}) of ground and ionic states of N-methylmaleimide.

Symmetry	Mode	S_0[a] B3LYP	S_0[b] Experiment	D_0[a] UB3LYP	Description[c]
a'	ν_1	3144	3103	3140	νC–H
	ν_2	3022	2930	2967	νH–H_3
	ν_3	2954	2903	2795	νC–H_3
	ν_4	1771	1751	1817	Symmetric νC=O
	ν_5	1592	1586	1534	νC=C
	ν_6	1458	1456	1400	δC–H_3
	ν_7	1422	1440	1315	δC–H_3
	ν_8	1369	1388	1169	Symmetric νC–N–C
	ν_9	1121	1150[d]	1116	rC–H_3
	ν_{10}	1103	1135	1007	νC–C+νN–CH_3
	ν_{11}	1018	1052	975	δC–H
	ν_{12}	811	832	836	γC–H
	ν_{13}	710	736	657	νC–C+νN–CH_3
	ν_{14}	608	633	601	Ring deformation
	ν_{15}	589	613	523	Ring deformation
	ν_{16}	367	389	339	δC=O
	ν_{17}	163	218[d]	211	γN–CH_3
	ν_{18}	138	168[e]	96	γC=O
a''	ν_{19}	3123	3080	3127	νC–H
	ν_{20}	3056	2963	3045	νC–H_3
	ν_{21}	1714	1701	1782	Asymmetric νC=O
	ν_{22}	1478	1475	1374	δC–H_3
	ν_{23}	1286	1336	1307	δC–H
	ν_{24}	1238	1254	1129	Asymmetric νC–N–C
	ν_{25}	1071	1108	1038	rC–H_3
	ν_{26}	937	958	944	γC–H
	ν_{27}	924	940	782	Ring deformation
	ν_{28}	752	770	618	Ring deformation
	ν_{29}	684	696	578	Ring deformation
	ν_{30}	553	574	551	δC=O
	ν_{31}	288	299[d]	244	γC=O
	ν_{32}	259	281[d]	239	δN–CH_3
	ν_{33}	71*i*	152[e]	69	τN–CH_3

[a]After scaling with factor 0.9676 (Ref. 49).
[b]IR frequencies reported by Parker (Ref. 50) except those labeled d and e, which have been obtained in the same study from Raman spectroscopy and inelastic neutron scattering, respectively.
[c]Description appropriate for S_0; ν=stretch; δ=in-plane bend; γ=out-of-plane bend; τ=torsion.

bands, the lowest one being a broad band with a first observable feature at about 3.5 eV and reaching its maximum at about 4.3 eV. It was assigned as the analog of the S_3 state in maleimide. The second band shows well-resolved vibrational transitions, and has its 0–0 transition at 44 623 cm^{-1} (5.53 eV).

Table VIII shows that more dramatic changes occur in the ionic manifold. Previously it was mentioned that the ground ionic state becomes the $X\,^2A'((\pi_N)^{-1})$ state for which vertical and adiabatic ionization energies of 10.074 and 9.812 eV, respectively, are calculated, their difference of 262 meV being one more reflection of the larger changes in geometry upon ionization. At the equilibrium geometry of the $X\,^2A'$ state we find that the $A^2A''((n_o^-)^{-1})$ state is 0.53 eV higher in energy. Separate calculations on this $A\,^2A''((n_o^-)^{-1})$ state at the UB3LYP/6-311+G* level show that it has a vertical and adiabatic ionization energy of 10.099 and 10.019 eV, respectively. The present calculations thus lead to the conclusion that with respect to maleimide a reversal of the two lower ionic states has taken place in N-methyl maleimide, but also that the two states remain close in energy.

The prediction that the $(\pi_N)^{-1}$ state is the ionic ground state of N-methyl maleimide is at odds with the conclusions

TABLE VIII. Description of the ground and lower-lying electronic singlet states of neutral N-methylmaleimide and of the ground and first excited states of its radical cation. For the neutral molecule excitation energies and oscillator strengths have been calculated by TD–DFT at the B3LYP/6-311+G* optimized S_0 ($1\,^1A'$) geometry; for the radical cation excitation energies have been calculated by TD–DFT at the UB3LYP/3-311+G* optimized geometry of the D_0 ($X\,^2A'$) state of the radical cation. The excitation energies between parentheses refer to a TD–DFT calculation at the UB3LYP/6-311+G* optimized S_0 ($1\,^1A'$) geometry using the orbitals of the D_0 ($X\,^2A'$) state.

State	Description	Energy (eV)	Oscillator strength
S_0 ($1\,^1A'$)	$(\pi_{C=C})^2(n_o^+)^2(\pi_N)^2(n_o^-)^2$	0	
S_1 ($2\,^1A'$)	$(\pi_{C=C})^2(n_o^+)^2(\pi_N)^2(n_o^-)^1(\pi^*_{C-C})^1$	3.45	0.0000
S_2 ($1\,^1A''$)	$(\pi_{C=C})^2(n_o^+)^2(\pi_N)^1(n_o^-)^2(\pi^*_{C-C})^1$	3.99	0.0077
S_3 ($2\,^1A''$)	$(\pi_{C=C})^2(n_o^+)^1(\pi_N)^2(n_o^-)^2(\pi^*_{C-C})^1$	4.17	0.0008
S_4 ($3\,^1A''$)	$(\pi_{C=C})^1(n_o^+)^2(\pi_N)^2(n_o^-)^2(\pi^*_{C-C})^1$	5.65	0.2813
D_0 ($X\,^2A'$)	$(\pi_{C=C})^2(n_o^+)^2(\pi_N)^1(n_o^-)^2$	0 (0.0)	
D_1 ($A\,^2A''$)	$(\pi_{C=C})^2(n_o^+)^2(\pi_N)^2(n_o^-)^1$	0.53 (0.0)	
D_2 ($B\,^2A'$)	$(\pi_{C=C})^2(n_o^+)^1(\pi_N)^2(n_o^-)^2$	1.55 (0.69)	
D_3 ($C\,^2A'$)	$(\pi_{C=C})^1(n_o^+)^2(\pi_N)^2(n_o^-)^2$	1.59 (0.87)	

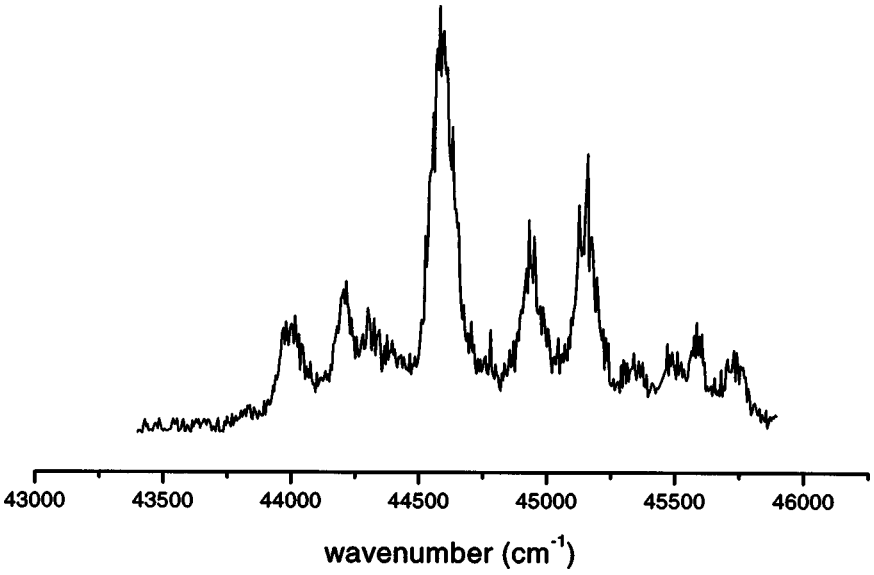

FIG. 5. (1+1) REMPI excitation spectrum of effusively introduced N-methyl maleimide.

reached by Robin[43] In that study it was initially remarked that the large difference between the first ionization potentials of N-methyl maleimide and maleic anhydride might be taken as an indication that ionization occurs from a π orbital rather than a lone pair, but this was later refuted on the basis of lone pair ionizations in simple acids and amides.[47] Although the ordering of the first two electronic ionization limits may therefore still be a matter of debate, this issue is less important for the interpretation of the photoelectron spectra obtained in the present study. It is clear, however, that the elucidation of the electronic structure of the radical cation would greatly benefit from additional He(I) photoionization studies.

In maleimide, considerable mixing occurred between the $(\pi_N)^{-1}$ and $(\pi_{C=C})^{-1}$ configurations. In N-methyl maleimide this mixing is nearly absent. At the equilibrium geometry of the $X\,^2A'$ state, the $C\,^2A'((\pi_{C=C})^{-1})$ state is calculated to have an excitation energy of 1.59 eV, but this is lowered to 0.87 eV at the equilibrium geometry of S_0. When we now consider the ionization routes of the various excited states in light of these calculations, we have to conclude that in N-methyl maleimide the situation is quite different from that in maleimide. Table VIII shows that in a one-configuration description of excited- and ionic states S_4 ionizes dominantly to D_3. The calculations predict that this pathway requires more energy than in maleimide, where S_4 could ionize to D_1 as a result of heavy mixing between the $(\pi_N)^{-1}$ and $(\pi_{C=C})^{-1}$ configurations. It might well be therefore that ionization to the parent ionic state of S_4 is energetically not possible in one-color REMPI experiments via S_4. On the other hand, on the basis of symmetry arguments we can also foresee that ionization of S_4 to the $X\,^2A'((\pi_N)^{-1})$ state becomes rapidly allowed beyond the one-configuration picture.

2. Multiphoton ionization and excited-state photoelectron spectroscopy

N-methyl maleimide has been investigated in the one-photon excitation region of 44 000–45 500 cm^{-1} under room temperature as well as supersonically cooled conditions. Previous absorption experiments[24] and our *ab initio* calculations lead us to believe that at these energies excitation of S_4 should take place. Figure 5 shows the (1+1) REMPI excitation spectrum obtained on effusively introduced N-methyl maleimide. The resonances observed in this spectrum are tabulated in Table IX, where the excitation energies reported for the vapor absorption spectrum are also given. Comparison of the two spectra shows that the absorption spectrum is shifted by 35 cm^{-1} to the blue with respect to the REMPI excitation spectrum. Some further remarks on the assignment of the bands in the spectrum are in order. The availability of the experimental frequencies in the ground state enables us to come to a straightforward assignment of the two strong hot bands, the other (broad) hot band 280 cm^{-1} below the origin transition probably consists of several transitions and cannot be assigned unambiguously. Previously, the 349 cm^{-1} band to the blue of the 0_0^0 transition was assigned as an overtone of a 182 cm^{-1} vibration.[24] In our opinion, this cannot be reconciled with the intensity of the higher overtones and with the intensities as measured in the present study. We

TABLE IX. Observed resonances in the (1+1) REMPI excitation spectrum of N-methyl maleimide of S_4 depicted in Fig. 5.

Excitation energy (cm^{-1})	Shift[a]	Assignment	Absorption[b]
43 995	−596	15_1^0	44 014
44 204	−387	16_1^0	44 228
~44 310	~280		44 346
44 591	0	0_0^0	44 623
44 940	349	16_0^1	44 984
45 152	561	15_0^1	45 188
45 330	739	13_0^1	45 372
45 493	902	$16_0^1 15_0^1$	45 537
45 587	996	11_0^1 or 10_0^1	45 620
45 728	1137	15_0^2	45 767

[a]Shift with respect to 0–0 transition.
[b]Absorption spectrum of N-methylmaleimide vapor reported by Seliskar and McGlynn (Ref. 24).

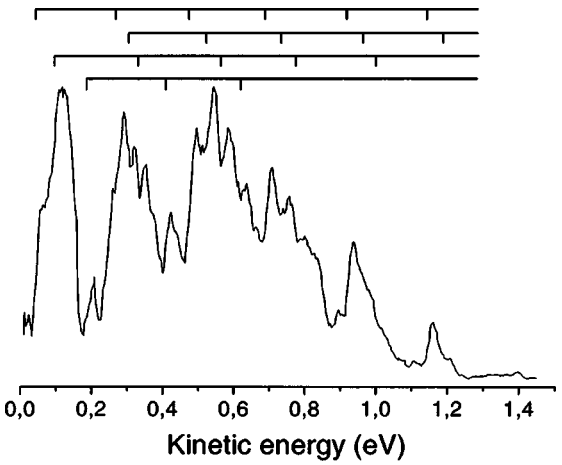

FIG. 6. Excited-state photoelectron spectrum of the vibrationless S_4 excited state of N-methyl maleimide excited at 44 590 cm^{-1}.

therefore reassign it to the 16_0^1 transition. Similarly, the weak 739 cm^{-1} band is reassigned to the 13_0^1 transition.

In order to get more detailed information on the spectroscopic and dynamic properties of the excited state, an excited-state photoelectron spectrum was measured at the maximum of the origin transition (44 590 cm^{-1}). This spectrum, shown in Fig. 6, was recorded employing effusively introduced N-methyl maleimide and at a relatively high laser power. Essentially the same spectra could be obtained under supersonically cooled conditions and at a lower laser power, but with a considerably worse signal-to-noise ratio. When trying to assign the photoelectron spectrum, one rapidly comes to the conclusion that the various peaks can be ordered in series involving average steps of 221 meV (1783 cm^{-1}). This frequency agrees nicely with the frequency calculated for the C═O stretch vibration ν_4^+ in the ionic ground state. The first series has a clear first member at 1.160 eV and goes up to five vibrational quanta of ν_4^+. A similar series seems to start at 1.211 eV and can be followed up to $\nu_4^+ = 4$. A third series is shifted by ~130 meV (~1100 cm^{-1}) from the first series, and, on the basis of Table VII, probably involves ionization to combination levels of $n\nu_4^+$ and $\nu_8^+ = 1$. The apparent first member of a last series involving ν_4^+ is seen at a photoelectron energy of 0.636 eV. Most probably, there are other members of this series at higher photoelectron energies, but they have too low an intensity, or are overlapped by other stronger bands. It is therefore not known on which mode this series is built.

For an absolute assignment we need to know where the $0''-0_0^+$ peak is located. One possible choice is to assign the 1.160 eV peak to the $0''-0_0^+$ peak and the 1.211 eV peak to a hot band, i.e., to an ionization process that starts in a vibrationally excited level of the ground state. This assignment implies that the adiabatic ionization energy to D_0 is 9.897 eV. The intensity distribution in the photoelectron spectrum suggests, however, that the whole assignment might also be shifted by one (or more) quanta of the C═O stretch vibration. The spectrum in Fig. 6 shows indeed a very small peak around 1.4 eV. If this peak is real—but the present experimental conditions do not allow us to make a decision on this—then the 1.160 and 1.182 eV peaks can be readily (re)assigned as the $\nu_5^+ = 1$ and $\nu_4^+ = 1$ peaks.

For maleimide, the photoelectron spectrum via S_4 showed two ionization routes. The dominant one involved ionization to one particular—in that case excited—ionic state with a propensity for conservation of vibrational energy. In the other one, high-lying vibrational levels of a lower-lying excited state were ionized to the ground ionic state, a process in which dispersal of vibrational energy occurred. The photoelectron spectrum in Fig. 6 is qualitatively different: one would, in fact, be led to conclude that all that is seen here is ionization to the ground ionic state. This might be due to the inaccessibility of the corresponding ionization continua of S_4 as suggested by the calculations, or to a larger dispersal of S_4 character over lower-lying electronic states, which is expected to be enhanced on account of the larger density of states introduced by the methyl substituent. Even without explicit assignment of the various peaks, it is clear that we deal here either with ionization involving very large changes in geometry, or ionization of one or more states with a large vibrational content. Based upon our interpretation of the maleimide spectrum, we conclude that the latter is the case.

The dominant activity of the C═O stretch vibration is another indication that the photoionization process of N-methyl maleimide via S_4 differs more than one would intuitively assume from its parent compound maleimide, where ionization to D_0 was accompanied by activity of the ring deformation mode ν_8 and the C═C stretch vibration ν_4. In principle, two explanations for this difference come to mind. A first explanation is that in maleimide S_4 is coupled to other states than in N-methyl maleimide. For maleimide we reached the conclusion that S_3 is most probably coupled to S_4; for N-methyl maleimide we would be talking about a state other than S_3 that undergoes large changes in the carbonyl bonds upon ionization. A second explanation is simply that the ground ionic state of the two molecules is different. Our calculations suggest that the second explanation is the correct one.

IV. CONCLUSIONS

We have investigated the spectroscopic and dynamic properties of the strongly one-photon absorbing $S_4(\pi_{C=C}\pi^*)$ state of maleimide and N-methyl maleimide. To this purpose, an experimental approach was combined with *ab initio* calculations of the electronic structure of the molecules. Experimentally, we have found that the wave function of the excited state can be probed in detail by projection on the ionic manifold using excited-state photoelectron spectroscopy. These experiments demonstrate that ionization of maleimide excited to S_4 occurs along several pathways. On the one hand, a channel has been identified that in a one-configuration picture can be described as ionization of the π^* electron from the $\pi_{C=C}\pi^*$ excited state. This channel leads to an electronically excited ionic state with an experimental excitation energy that is in excellent agreement with the *ab initio* predicted one. The experiments show as well that the ionization process populates a broad range of vibrational levels in the ionic ground state, which

can only be explained if we go beyond the one-configuration picture. On the basis of *ab initio* calculated displacement parameters between various excited states and the ionic ground state, it has been argued that the observed Franck–Condon pattern demonstrates that an electronic state is ionized that does not only contain S_4 character but also that of lower-lying states, in particular that of the $S_3(\pi_N\pi^*)$ state.

Our experiments and calculations demonstrate that N-methyl substitution of the molecule leads to large changes, in particular for the ionic manifold where the ground ionic state is now calculated to be associated with the $(\pi_N)^{-1}$ configuration as opposed to the $(n_o^-)^{-1}$ configuration in maleimide. This prediction is in excellent agreement with the dominant activity of the C═O stretch vibration seen in excited-state photoelectron spectra of S_4. In contrast to maleimide, these spectra do not show clearly multiple ionization pathways, although the observed Franck–Condon pattern strongly suggests a dominant role of internal conversion.

Until the present study, the ionic manifold of the two molecules was virtually unexplored. Apart from elucidating the composition and properties of the S_4 state, the present experiments have also enabled us to obtain information on the spectroscopic properties of this manifold in the form of ionization energies and vibrational frequencies.

ACKNOWLEDGMENTS

The authors wish to thank Ing. D. Bebelaar for valuable experimental assistance, and Professor C. A. de Lange and Professor M. Glasbeek for use of equipment.

[1] D. H. A. ter Steege, A. C. Wirtz, and W. J. Buma, J. Chem. Phys. **116**, 1 (2002).
[2] D. H. A. ter Steege, C. Lagrost, and W. J. Buma, J. Chem. Phys. **117**, 8270 (2002).
[3] V. Blanchet, M. Z. Zgierski, and A. Stolow, J. Chem. Phys. **114**, 1194 (2001).
[4] M. Schmitt, S. Lochbrunner, J. P. Shaffer, J. J. Larsen, M. Z. Zgierski, and A. Stolow, J. Chem. Phys. **114**, 1206 (2001).
[5] S.-H. Lee, K.-C. Tang, I.-C. Chen, M. Schmitt, J. P. Schaffer, T. Schultz, J. G. Underwood, M. Z. Zgierski, and A. Stolow, J. Phys. Chem. A **106**, 8979 (2002).
[6] R. A. Rijkenberg, W. J. Buma, C. A. van Walree, and L. W. Jenneskens, J. Phys. Chem. A **106**, 5249 (2002).
[7] C. E. Hoyle, K. Viswanathan, S. C. Clark, C. W. Miller, C. Nguyen, S. Jönsson, and L. Shao, Macromolecules **32**, 2793 (1999).
[8] M. Shimose, C. E. Hoyle, S. Jönssen, P. E. Sundell, J. Owens, and K. Vaughn, Polym. Prepr. (Am. Chem. Soc. Div. Polym. Chem.) **36**, 485 (1995).
[9] S. Jönsson, P. E. Sundell, J. Hultgren, D. Sheng, and C. E. Hoyle, Prog. Org. Coat. **27**, 107 (1996).
[10] C. Decker, F. Morel, S. C. Clark, S. Jönssen, and C. E. Hoyle, Polym. Mater. Sci. Eng. **75**, 198 (1996).
[11] H. Andersson, U. W. Gedde, and A. Hult, Macromolecules **29**, 1649 (1996).
[12] H. Andersson, U. W. Gedde, and A. Hult, J. Coat. Technol. **69**, 91 (1997).
[13] C. E. Hoyle, S. C. Clark, S. Jönssen, and M. Shimose, Polymer **38**, 5695 (1997).
[14] S. Jönssen, P. E. Sundell, M. Shimose, S. C. Clark, C. Miller, F. Morel, C. Decker, and C. E. Hoyle, Nucl. Instrum. Methods Phys. Res. B **131**, 276 (1997).
[15] P. Kohli, A. B. Scranton, and G. J. Blanchard, Macromolecules **31**, 5681 (1998).
[16] C. E. Hoyle, S. C. Clark, S. Jönssen, and M. Shimose, Polym. Commun. **38**, 5695 (1998).
[17] C. W. Miller, S. Jönssen, C. E. Hoyle, C. Hasselgren, T. Haraldson, and L. Shao, RadTech'98 Proc. 182 (1998).
[18] J. von Sonntag and W. Knolle, J. Photochem. Photobiol., A **136**, 133 (2000).
[19] S. C. Clark, Ph.D. dissertation, Department of Polymer Science, The University of Southern Mississippi, Hattiesburg, MS, 1999.
[20] J. von Sonntag, Ph.D. dissertation, Faculty of Chemistry and Mineralogy, The University of Leipzig, Germany, 1999.
[21] J. M. Warman, R. D. Abellon, H. J. Verhey, J. W. Verhoeven, and J. W. Hofstraat, J. Phys. Chem. B **101**, 4913 (1997).
[22] B. Kükrer Kaletas, R. M. Williams, B. König, and L. De Cola, Chem. Commun. (Cambridge) **2002**, 776.
[23] T. Matsuo, Bull. Chem. Soc. Jpn. **38**, 557 (1965).
[24] C. J. Seliskar and S. P. McGlynn, J. Phys. Chem. **55**, 4337 (1971).
[25] C. J. Seliskar and S. P. McGlynn, J. Phys. Chem. **56**, 275 (1972).
[26] C. J. Seliskar and S. P. McGlynn, J. Phys. Chem. **56**, 1471 (1972).
[27] C. R. Scheper, W. J. Buma, and C. A. de Lange, J. Electron Spectrosc. Relat. Phenom. **109**, 8319 (1998).
[28] A. M. Rijs, E. H. G. Backus, C. A. de Lange, N. P. C. Westwood, and M. H. M. Janssen, J. Electron Spectrosc. Relat. Phenom. **112**, 151 (2000).
[29] P. Kruit and F. H. Read, J. Phys. E **16**, 313 (1983).
[30] C. E. Moore, *Atomic Energy Levels*, Natl. Bur. Stand. (U.S.) Circ. No. 35 (U.S. GPO, Washington, DC, 1971), Vol. II.
[31] M. J. Frisch, G. W. Trucks, H. B. Schlegel *et al.*, GAUSSIAN 98, Revision A.5; Gaussian, Inc., Pittsburgh, PA, 1998.
[32] M. W. Schmidt, K. K. Baldridge, J. A. Boatz *et al.*, J. Comput. Chem. **14**, 1347 (1993).
[33] W. J. Buma and F. Zerbetto, J. Chem. Phys. **103**, 10492 (1995).
[34] E. V. Doktorov, I. A. Malkin, and V. I. Man'ko, J. Mol. Spectrosc. **64**, 302 (1977).
[35] R. A. Rijkenberg and W. J. Buma, J. Phys. Chem. A **106**, 3727 (2002).
[36] M. J. Frisch, J. A. Pople, and J. S. Binkley, J. Chem. Phys. **80**, 3265 (1984).
[37] J. B. Foresman, M. Head-Gordon, J. A. Pople, and M. J. Frisch, J. Phys. Chem. **96**, 135 (1992).
[38] A. M. Becke, J. Chem. Phys. **98**, 5648 (1993).
[39] L. Harsanyi, E. Vajda, and I. Hargittai, J. Mol. Struct. **129**, 315 (1985).
[40] T. Wolbaek, P. Klaboe, and C. J. Nielsen, J. Mol. Struct. **27**, 283 (1975).
[41] T. Wolbaek, P. Klaboe, and C. J. Nielsen, J. Mol. Struct. **28**, 269 (1975).
[42] A. J. Barnes, L. Le Gall, C. Madec, and J. Lauransan, J. Mol. Struct. **38**, 109 (1977).
[43] M. B. Robin, *Higher Excited States of Polyatomic Molecules* (Academic, New York, 1975), Vol. II.
[44] P. M. Weber and N. Thantu, Chem. Phys. Lett. **197**, 556 (1992).
[45] B. Kim, C. P. Schick, and P. M. Weber, J. Chem. Phys. **103**, 6903 (1995).
[46] S. Hillenbrand, L. Zhu, and P. Johnson, J. Chem. Phys. **92**, 870 (1990).
[47] C. R. Brundle, D. W. Turner, M. B. Robin, and H. Basch, Chem. Phys. Lett. **3**, 292 (1969).
[48] P. J. Cox and S. F. Parker, Acta Crystallogr., Sect. C: Cryst. Struct. Commun. **52**, 2578 (1996).
[49] A. P. Scott and L. Radon, J. Phys. Chem. **100**, 16502 (1996).
[50] S. F. Parker, Spectrochim. Acta, Part A **51**, 2067 (1995).